

# Thermal Radiation Effects on the Flow by an Exponentially Stretching Surface: a Series Solution

Sohail Nadeem<sup>a</sup>, Tasawar Hayat<sup>a,b</sup>, Muhammad Yousaf Malik<sup>a</sup>, and Saeed Ahmed Rajput<sup>a</sup>

<sup>a</sup> Department of Mathematics, Quaid-i-Azam University 45320, Islamabad 44000, Pakistan

<sup>b</sup> Department of Mathematics, Colledge of Sciences, King Saud University, P. O. Box 2455, Riyadh 11451 Saudi Arabia

Reprint requests to S. N.; E-mail: snqau@hotmail.com

Z. Naturforsch. **65a**, 495 – 503 (2010); received January 19, 2009 / revised July 14, 2009

This article analytically describes the thermal radiation effects on the flow and heat transfer characteristics. The flow in a second-grade fluid is created due to an exponentially porous stretching surface. The series solutions of velocity and temperature are developed by a homotopy analysis method. The heat transfer results are obtained for the two cases, namely, (i) the prescribed exponential order surface temperature (PEST) and (ii) the prescribed exponential order heat flux (PEHF). It is noticed that the temperature profile in both cases decreases when radiation parameter is increased.

*Key words:* Second-Grade Fluid; Porous Stretching Surface; Series Solutions.

## 1. Introduction

The last several decades have shown an increasing amount of attention to the problem of non-Newtonian fluids. This is infact due to their increasing use in industry. A very important type of non-Newtonian fluid is the differential type fluid. There is a simplest subclass of these fluids known as second-grade fluids that has led to a considerable interest among researchers, seen in a vast literature presently. The constitutive equation of second-grade fluid can describe the normal stress effects. However, such an equation does not explain the shear thinning/shear thickening effects. Moreover, the equations of second grade in general are more nonlinear and of higher order than the Navier-Stokes equations [1–3]. Extensive literature dealing with the flows of second-grade fluids exists in various geometries, with and without heat transfer and porous media. However, some recent investigations [4–14] shed light on the interesting flows of second-grade fluids. It is worth mentioning that over the past four decades, the flow due to a stretching surface has occupied a fundamental place in many engineering applications, such as continuous coating, rolling, and extrusion in manufacturing process, the boundary layer along a film in condensation process, and aerodynamic extrusion of plastic sheet. Since the pioneering works of Sakiadis [15, 16], various examined effects of the

problem are seen in the recent studies [17–25]. In [26], Khan and Sanjayanand studied the flow and heat transfer characteristics in a second-grade fluid bounded by an exponentially stretching surface. The energy equation in a viscous fluid is selected.

The object of the present work is to extend the analysis of [26] into three directions. Firstly, to model the energy equation in a second-grade fluid. Secondly, to consider a porous stretching surface. Thirdly, to derive a series solution by a homotopy analysis method (HAM) [27–40]. The paper is divided into five sections. Section 2 contains the mathematical formulation, the series solution of temperature and velocity are demonstrated in Section 3. Discussion of the graph is presented in Section 4, whereas Section 5 includes the main conclusions.

## 2. Formulation of the Problem

We consider the two-dimensional flow of a second-grade fluid bounded by a porous stretching surface. The moving surface has an axial velocity of exponential order in axial distance, i. e.  $U_0 \exp[x/2]$ . The flow and heat transfer characteristics can be described by the following equations:

$$\frac{\partial u}{\partial x} + \frac{\partial v}{\partial y} = 0, \quad (1)$$

$$u \frac{\partial u}{\partial x} + v \frac{\partial u}{\partial y} = \gamma \frac{\partial^2 u}{\partial y^2} - k_0 \left\{ u \frac{\partial^3 u}{\partial x \partial y^2} + v \frac{\partial^3 u}{\partial y^3} - \frac{\partial u}{\partial y} \frac{\partial^2 u}{\partial x \partial y} + \frac{\partial u}{\partial x} \frac{\partial^2 u}{\partial y^2} \right\}, \tag{2}$$

$$u \frac{\partial T}{\partial x} + v \frac{\partial T}{\partial y} = \alpha \frac{\partial^2 T}{\partial y^2} + \frac{\mu}{\rho c_p} \left( \frac{\partial u}{\partial y} \right)^2 - k_0 \frac{\partial u}{\partial y} \frac{\partial}{\partial y} \left( u \frac{\partial u}{\partial x} + v \frac{\partial v}{\partial y} \right) - \frac{\partial q_r}{\partial y}, \tag{3}$$

where radiation effects are included,  $(u, v)$  are the velocity components in the  $(x, y)$  directions,  $\rho$  is the fluid density,  $\gamma$  is the kinematic viscosity,  $k_0 = -\alpha_1/\rho$  ( $\alpha_1 < 0$ ) is the elastic parameter in a second-grade fluid,  $T$  is the temperature,  $\alpha$  is the thermal diffusibility,  $c_p$  is the specific heat at constant pressure and  $q_r$  is the radiative heat flux. Fosdick and Rajagopal [41] have discussed the case of a second-order fluid and found that the following relations hold:

$$\mu \geq 0, \quad \alpha_1 \leq 0, \quad \alpha_1 + \alpha_2 \neq 0.$$

The boundary conditions are chosen as

$$\begin{aligned} u &= U_w(x) = U_0 \exp\left(\frac{x}{l}\right), \quad v = -\beta, \\ T &= T_w \text{ at } y = 0, \\ u &= 0, \quad u_y = 0, \quad T = T_\infty \text{ as } y \rightarrow \infty, \end{aligned} \tag{4}$$

in which  $T_w$  and  $T_\infty$  are the temperature of the sheet and the ambient fluid, respectively, and the constant  $\beta$  is the suction and the injection velocity of the stretching surface when  $\beta > 0$  and  $\beta < 0$ , respectively. Here  $\beta = 0$  represents the impermeability of the surface. By Rosseland approximation [42] it is

$$q_r = -\frac{4\sigma^*}{3k^*} \frac{\partial T^4}{\partial y}. \tag{5}$$

Here  $\sigma^+$  is the Stefan-Boltzmann constant,  $k^*$  is the absorption coefficient and the Taylor series gives

$$T^4 = 4T_\infty^3 T - 3T_\infty^4. \tag{6}$$

From (3), (5), and (6) we can write

$$\begin{aligned} u \frac{\partial T}{\partial x} + v \frac{\partial T}{\partial y} &= \left( \alpha + \frac{4\sigma^* T_\infty^4}{3k^* \rho c_p} \right) \frac{\partial^2 T}{\partial y^2} \\ &+ \frac{\mu}{\rho c_p} \left( \frac{\partial u}{\partial y} \right)^2 - k_0 \frac{\partial u}{\partial y} \frac{\partial}{\partial y} \left( u \frac{\partial u}{\partial x} + v \frac{\partial v}{\partial y} \right). \end{aligned} \tag{7}$$

We are interested in finding the solution of the above equation in the following two cases:

- (i) with prescribed exponential order surface temperature (PEST) and
- (ii) with prescribed exponential order heat flux (PEHF).

For the above two cases, the corresponding boundary conditions are as follows:

$$T = T_w = T_\infty + T_0 \exp\left(\frac{v_0 x}{l}\right) \text{ at } y = 0 \tag{8}$$

for the PEST case and

$$-k \left( \frac{\partial T}{\partial y} \right)_w = T_1 \exp\left(\frac{v_1 + 1}{2l} x\right) \text{ at } y = 0 \tag{9}$$

for the PEHF case,

and

$$T \rightarrow T_\infty \text{ as } y \rightarrow \infty, \tag{10}$$

where  $T_w$  and  $T_1$  are wall temperatures,  $T_\infty$  is the temperature of the ambient fluid,  $v_0$ ,  $v_1$ , and  $T_0$  are constants.

Introducing

$$\begin{aligned} u &= U_0 \exp\left(\frac{x}{l}\right) f'(\eta), \\ v &= -\sqrt{\frac{\gamma U_0}{2l}} \exp\left(\frac{x}{l}\right) \{f(\eta) + \eta f'(\eta)\}, \end{aligned} \tag{11}$$

$$\eta = y \sqrt{\frac{U_0}{2\gamma l}} \exp\left(\frac{x}{2l}\right),$$

$$T = T_\infty + T_0 \exp\left(\frac{x}{2l}\right) \theta(\eta) \tag{12}$$

for the PEST case and

$$T = T_\infty + \frac{T_1}{k} \sqrt{\frac{2\gamma l}{U_0}} \exp\left(\frac{v_1 x}{2l}\right) g(\eta) \tag{13}$$

for the PEHF case.

The resulting problems reduce to

$$\begin{aligned} 2f_\eta^2 - ff_\eta\eta &= f_\eta\eta\eta \\ -k_1^* \left[ 3f_\eta f_\eta\eta\eta - \frac{1}{2}ff_\eta\eta\eta\eta - \frac{3}{2}f_\eta^2\eta\eta \right], \end{aligned} \tag{14}$$

$$\begin{aligned} f &= -v_w, \quad f_\eta = 1 \text{ at } \eta = 0, \\ f_\eta &= 0 \text{ as } \eta \rightarrow \infty, \end{aligned} \tag{15}$$

$$\begin{aligned} \theta_\eta\eta \left( 1 + \frac{4R}{3} \right) &+ Pr(f\theta_\eta - v_0 f_\eta \theta) \\ &= -PrE \left[ f_\eta^2\eta - \frac{k_1^*}{2} f_\eta\eta \{3f_\eta\eta f_\eta - f_\eta\eta\eta f\} \right], \end{aligned} \tag{16}$$

$$\theta(0) = 1, \tag{17}$$

$$\theta(\infty) = 0, \tag{18}$$

$$g_{\eta\eta} \left( 1 + \frac{4R}{3} \right) + Pr(fg_{\eta} - v_1 f_{\eta} g) = -PrE \left[ f_{\eta\eta}^2 - \frac{k_1^*}{2} f_{\eta\eta} \{ 3f_{\eta\eta} f_{\eta} - f_{\eta\eta\eta} f \} \right], \tag{19}$$

$$g_{\eta}(0) = -1, \tag{20}$$

$$g(\infty) = 0. \tag{21}$$

In the above equations  $f$  is the dimensionless stream function,  $k_1^* = k_0 U_w / \gamma l$  is the dimensionless viscoelastic parameter, and  $v_w$  is the dimensionless suction and injection parameter,  $Pr = \gamma / \alpha$  is the Prandtl number,  $E = \frac{U_0^2}{c_p T_0} \left( \frac{U_w}{U_0} \right)^{\left( \frac{4-v_0}{2} \right)}$ ,  $E = \frac{kU_0^2}{c_p T_1 \sqrt{\frac{2\gamma}{U_0}}} \left( \frac{U_w}{U_0} \right)^{\left( \frac{4-v_0}{2} \right)}$ , are the respective Eckert numbers for both the cases PEST and PEHF, and  $R = 4\sigma^* T_{\infty}^3 / kk^*$  is the radiation parameter.

### 3. Solution by Homotopy Analysis Method

For both PEST and PEHF cases, the initial guesses and the linear operators  $L_i$  ( $i = 1-3$ ) are [43–45]

$$f_0(\eta) = 1 - e^{-\eta}, \quad \theta_0(\eta) = e^{-\eta}, \quad g_0(\eta) = e^{-\eta}, \tag{22}$$

$$\Delta_1(f) = f''' - f', \quad \Delta_2 = f'' - f, \quad \Delta_3 = f'' - f. \tag{23}$$

The operators satisfy the following properties:

$$\Delta_1(f)[c_1 e^{-\eta} + c_2 e^{\eta} + c_3] = 0, \tag{24}$$

$$\Delta_2(f)[c_4 e^{-\eta} + c_5 e^{\eta}] = 0, \tag{25}$$

$$\Delta_3(f)[c_6 e^{-\eta} + c_7 e^{\eta}] = 0, \tag{26}$$

$c_1 - c_7$  are constants. From (14), (16), and (19), we can define the following zeroth-order deformation problems:

$$(1-p)\Delta_1[\hat{f}(\eta, p) - f_0(\eta)] = p\hbar_1 H_1 \tilde{N}_1[\hat{f}(\eta, p)], \tag{27}$$

$$(1-p)\Delta_2[\hat{\theta}(\eta, p) - \theta_0(\eta)] = p\hbar_2 H_2 \tilde{N}_2[\hat{\theta}(\eta, p)], \tag{28}$$

$$(1-p)\Delta_3[\hat{g}(\eta, p) - g_0(\eta)] = p\hbar_3 H_3 \tilde{N}_3[\hat{g}(\eta, p)], \tag{29}$$

$$\hat{f}(0, p) = v_w, \quad \hat{f}'(0, p) = 1, \quad \hat{f}'(\infty, p) = 0, \tag{30}$$

$$\hat{\theta}(0, p) = 1, \quad \hat{\theta}(\infty, p) = 0, \tag{31}$$

$$\hat{g}'(0, p) = -1, \quad \hat{g}(\infty, p) = 0. \tag{32}$$

In (27) to (29),  $\hbar_1, \hbar_2,$  and  $\hbar_3$  denote the non-zero auxiliary parameters,  $H_1, H_2,$  and  $H_3$  are the non-zero auxiliary functions, and

$$\begin{aligned} \tilde{N}_1[f(\eta, p)] &= 2 \left( \frac{\partial f}{\partial \eta} \right)^2 - f \frac{\partial^2 f}{\partial \eta^2} \\ &= \frac{\partial^3 f}{\partial \eta^3} - k_1^* \left[ 3 \frac{\partial f}{\partial \eta} \frac{\partial^3 f}{\partial \eta^3} - \frac{1}{2} f \frac{\partial^4 f}{\partial \eta^4} - \frac{3}{2} \left( \frac{\partial^2 f}{\partial \eta^2} \right)^2 \right], \end{aligned} \tag{33}$$

$$\begin{aligned} \tilde{N}_2[\theta(\eta, p)] &= \frac{\partial^2 \theta}{\partial \eta^2} \left( 1 + \frac{4R}{3} \right) + Pr \left( f \frac{\partial \theta}{\partial \eta} - v_0 \frac{\partial f}{\partial \eta} \theta \right) \\ &= -PrE \left[ \left( \frac{\partial^2 f}{\partial \eta^2} \right)^2 - \frac{k_1^*}{2} \frac{\partial^2 f}{\partial \eta^2} \left\{ 3 \frac{\partial f}{\partial \eta} \frac{\partial^2 f}{\partial \eta^2} - f \frac{\partial^3 f}{\partial \eta^3} \right\} \right], \end{aligned} \tag{34}$$

$$\begin{aligned} \tilde{N}_3[\theta(\eta, p)] &= \frac{\partial^2 g}{\partial \eta^2} \left( 1 + \frac{4R}{3} \right) + Pr \left( f \frac{\partial g}{\partial \eta} - v_1 \frac{\partial f}{\partial \eta} g \right) \\ &= -PrE \left[ \left( \frac{\partial^2 f}{\partial \eta^2} \right)^2 - \frac{k_1^*}{2} \frac{\partial^2 f}{\partial \eta^2} \left\{ 3 \frac{\partial f}{\partial \eta} \frac{\partial^2 f}{\partial \eta^2} - f \frac{\partial^3 f}{\partial \eta^3} \right\} \right]. \end{aligned} \tag{35}$$

Obviously,

$$\hat{f}(\eta, 0) = f_0(\eta), \quad \hat{f}(\eta, 1) = f(\eta), \tag{36}$$

$$\hat{\theta}(\eta, 0) = \theta_0(\eta), \quad \hat{\theta}(\eta, 1) = \theta(\eta), \tag{37}$$

$$\hat{g}(\eta, 0) = g_0(\eta), \quad \hat{g}(\eta, 1) = g(\eta). \tag{38}$$

When  $p$  varies from 0 to 1, then  $\hat{f}(\eta, p), \hat{\theta}(\eta, p), \hat{g}(\eta, p)$  vary from the initial guess  $f_0(\eta), \theta_0(\eta),$  and  $g_0(\eta),$  respectively. Considering that the auxiliary parameters  $\hbar_1, \hbar_2,$  and  $\hbar_3$  are so properly chosen that the Taylor series of  $\hat{f}(\eta, p), \hat{\theta}(\eta, p),$  and  $\hat{g}(\eta, p)$  expanded with respect to an embedding parameter converge at  $p = 1.$  Hence, (36) to (38) become

$$\hat{f}(\eta, p) = f_0(\eta) + \sum_{m=1}^{\infty} f_m(\eta) p^m, \tag{39}$$

$$\hat{\theta}(\eta, p) = \theta_0(\eta) + \sum_{m=1}^{\infty} \theta_m(\eta) p^m, \tag{40}$$

$$\hat{g}(\eta, p) = g_0(\eta) + \sum_{m=1}^{\infty} g_m(\eta)p^m, \tag{41}$$

$$f_m(\eta) = \left( \frac{1}{m!} \frac{\partial^m f(\eta, p)}{\partial p^m} \right)_{p=0}, \tag{42}$$

$$\theta_m(\eta) = \left( \frac{1}{m!} \frac{\partial^m \theta(\eta, p)}{\partial p^m} \right)_{p=0}, \tag{43}$$

$$g_m(\eta) = \left( \frac{1}{m!} \frac{\partial^m \hat{g}(\eta, p)}{\partial p^m} \right)_{p=0}. \tag{44}$$

The  $m$ th-order problems are satisfied by the following equations:

$$\Delta_1[f_m(\eta) - \chi_m f_{m-1}(\eta)] = \tilde{h}_1 \check{R}_m^1(\eta), \tag{45}$$

$$\Delta_2[\theta_m(\eta) - \chi_m \theta_{m-1}(\eta)] = \tilde{h}_2 \check{R}_m^2(\eta), \tag{46}$$

$$\Delta_3[g_m(\eta) - \chi_m g_{m-1}(\eta)] = \tilde{h}_3 \check{R}_m^3(\eta), \tag{47}$$

$$f_m(0) = f'_m(0) = f'_m(\infty) = 0, \tag{48}$$

$$\theta_m(0) = \theta_m(\infty) = 0, \tag{49}$$

$$g'_m(0) = g_m(\infty) = 0, \tag{50}$$

$$\begin{aligned} \check{R}_m^1(\eta) = & f''_{m-1}(\eta) \\ & - k_1^* \sum_{k=0}^{m-1} \left[ 3f'_{m-1-k} f'_k - \frac{1}{2} f_{m-1-k} f''_k - \frac{3}{2} f''_{m-1-k} f'_k \right] \\ & + \sum_{k=0}^{m-1} f_{m-1-k} f'_k - 2 \sum_{k=0}^{m-1} f'_{m-1-k} f'_k, \end{aligned} \tag{51}$$

$$\begin{aligned} \check{R}_m^2(\eta) = & \theta''_{m-1} \left( 1 + \frac{4R}{3} \right) \\ & + Pr \sum_{k=0}^{m-1} \{ f_{m-1-k} \theta'_k - v_0 f'_{m-1-k} \theta_k \} \\ & + EPr \left[ \sum_{k=0}^{m-1} f''_{m-1-k} f'_k - \frac{k_1^*}{2} \left\{ 3 \sum_{k=0}^{m-1} f''_{m-1-k} \sum_{k=0}^{m-1} f''_{m-1-k} f_k \right. \right. \\ & \left. \left. - \sum_{k=0}^{m-1} f'''_{m-1-k} \sum_{k=0}^{m-1} f''_{m-1-k} f_k \right\} \right], \end{aligned} \tag{52}$$

$$\begin{aligned} \check{R}_m^3(\eta) = & g''_{m-1} \left( 1 + \frac{4R}{3} \right) \\ & + Pr \sum_{k=0}^{m-1} \{ f_{m-1-k} g'_k - v_0 f'_{m-1-k} g_k \} \\ & + EPr \left[ \sum_{k=0}^{m-1} f''_{m-1-k} f'_k - \frac{k_1^*}{2} \left\{ 3 \sum_{k=0}^{m-1} f''_{m-1-k} \sum_{k=0}^{m-1} f''_{m-1-k} f_k \right. \right. \\ & \left. \left. - \sum_{k=0}^{m-1} f'''_{m-1-k} \sum_{k=0}^{m-1} f''_{m-1-k} f_k \right\} \right]. \end{aligned} \tag{53}$$

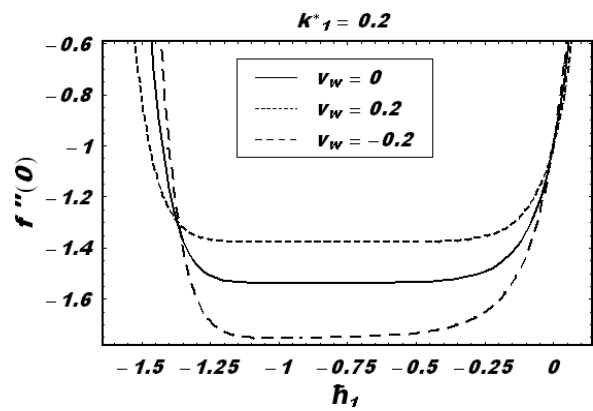


Fig. 1.  $\tilde{h}$ -curves for velocity profile and temperature profile.

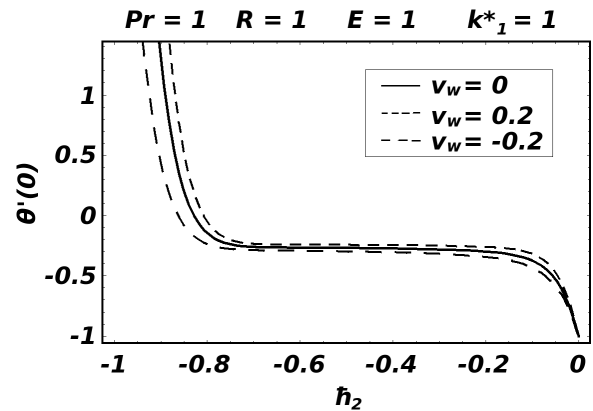


Fig. 2.  $\tilde{h}$ -curves for velocity profile and temperature profile.

Employing the Mathematica software, (45) to (50) have the following solutions:

$$\begin{aligned} f(\eta) = & \sum_{m=0}^{\infty} f_m(\eta) = \\ \lim_{M \rightarrow \infty} & \left[ \sum_{m=0}^M a_{m,0}^0 + \sum_{n=1}^{M+1} e^{-n\eta} \left( \sum_{m=n-1}^M \sum_{k=0}^{m+1-n} a_{m,n}^k \eta^k \right) \right], \end{aligned} \tag{54}$$

$$\begin{aligned} \theta(\eta) = & \sum_{m=0}^{\infty} \theta_m(\eta) = \\ \lim_{M \rightarrow \infty} & \left[ \sum_{n=1}^{M+1} e^{-n\eta} \left( \sum_{m=n-1}^M \sum_{k=0}^{m+1-n} A_{m,n}^k \eta^k \right) \right], \end{aligned} \tag{55}$$

$$\begin{aligned} g(\eta) = & \sum_{m=0}^{\infty} g_m(\eta) = \\ \lim_{M \rightarrow \infty} & \left[ \sum_{n=1}^{M+1} e^{-n\eta} \left( \sum_{m=n-1}^M \sum_{k=0}^{m+1-n} F_{m,n}^k \eta^k \right) \right], \end{aligned} \tag{56}$$

in which  $a_{m,0}^0, a_{m,n}^k, A_{m,n}^k, F_{m,n}^k$  are constants and can be determined easily by adopting a procedure in [29].

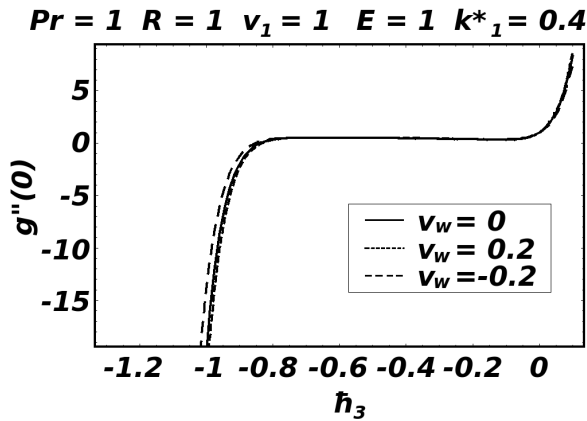


Fig. 3.  $h$ -curves for velocity profile and temperature profile.

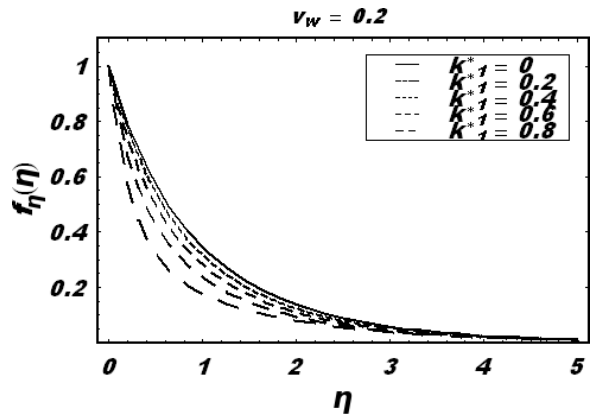


Fig. 6. Velocity profile  $f_\eta(\eta)$  with  $v_w = 0.2$  for different values of  $k_1^*$ .

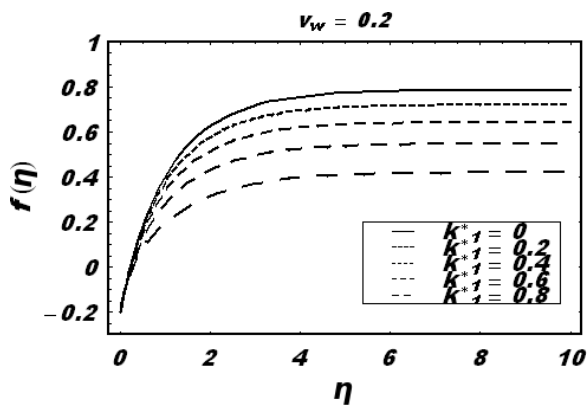


Fig. 4. Velocity profile  $f(\eta)$  with  $v_w = 0.2$  for different values of  $k_1^*$ .

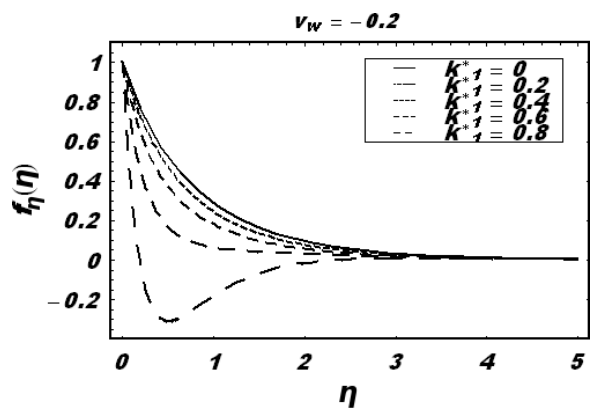


Fig. 7. Velocity profile  $f_\eta(\eta)$  with  $v_w = -0.2$  for different values of  $k_1^*$ .

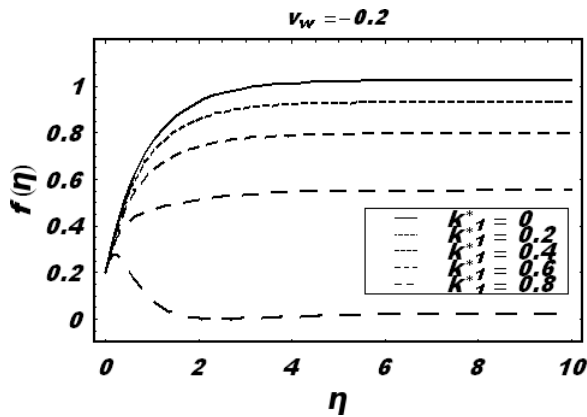


Fig. 5. Velocity profile  $f(\eta)$  with  $v_w = -0.2$  for different values of  $k_1^*$ .

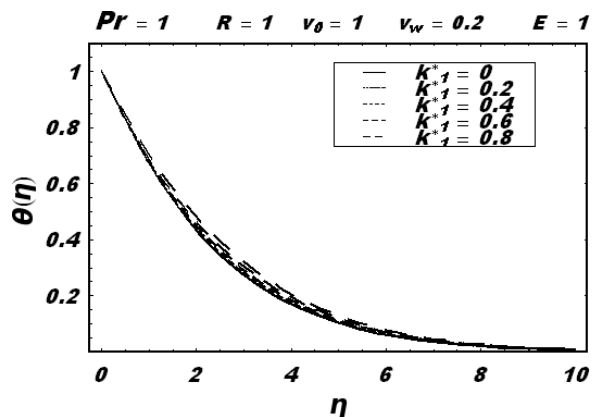


Fig. 8. Temperature profile in PEST case for different values of  $k_1^*$ .

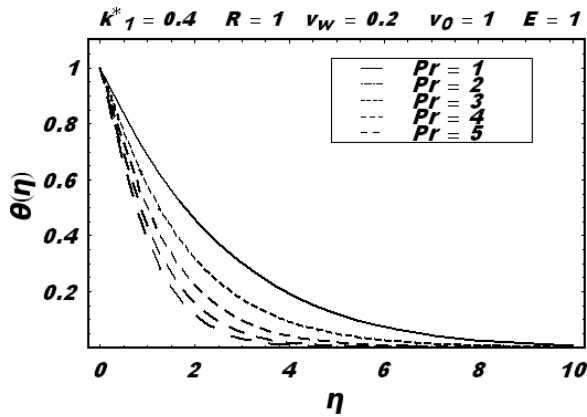


Fig. 9. Temperature profile in PEST case for different values of  $k_1^*$ .

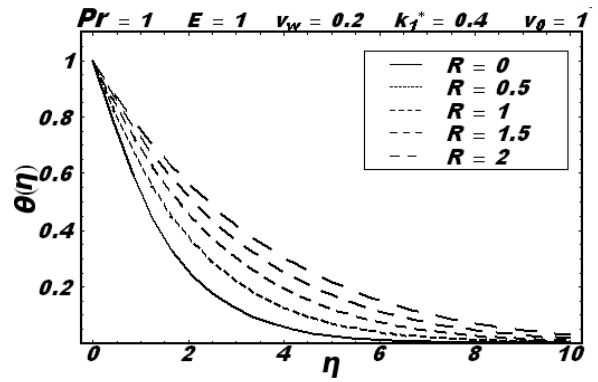


Fig. 12. Temperature profile in PEST case with  $v_w = 0.2$  for different values of radiation parameter  $R$ .

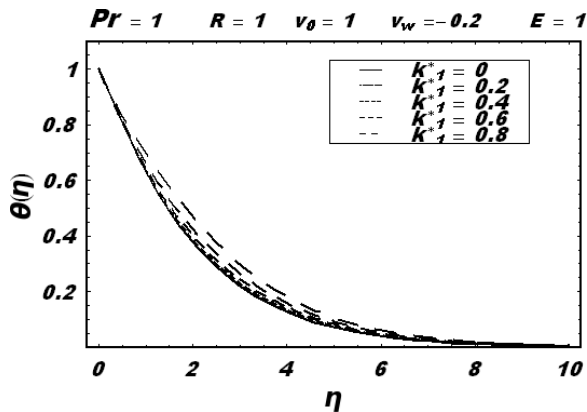


Fig. 10. Temperature profile in PEST case for different values of  $Pr$ .

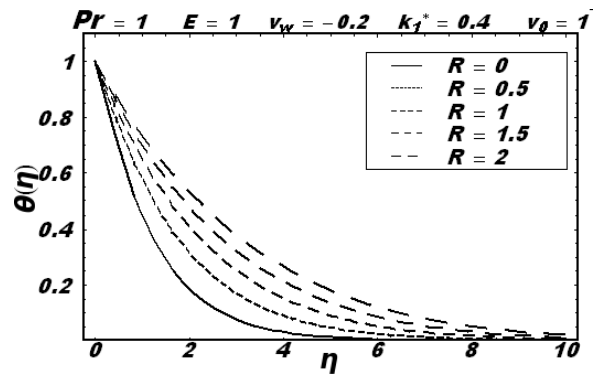


Fig. 13. Temperature profile in PEST case with  $v_w = -0.2$  for different values of radiation parameter  $R$ .

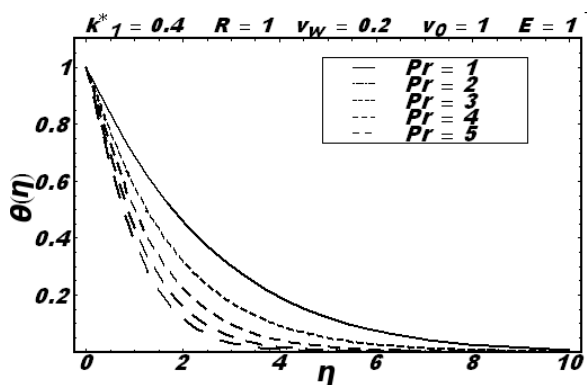


Fig. 11. Temperature profile in PEST case for different values of  $Pr$ .

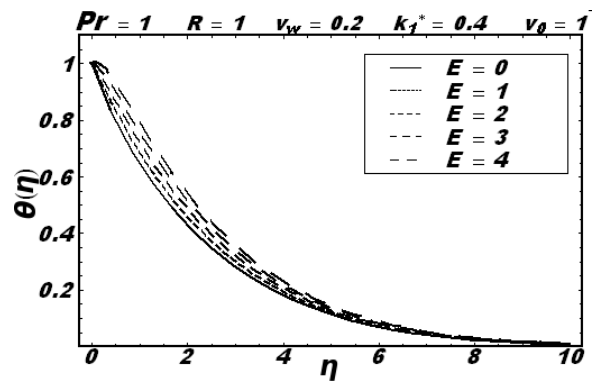


Fig. 14. Temperature profile in PEST case with  $v_w = 0.2$  for different values of  $E$ .

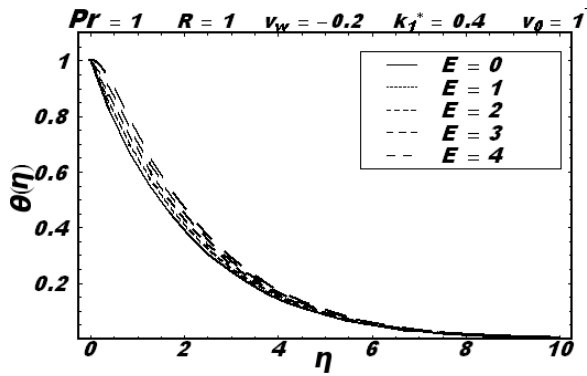


Fig. 15. Temperature profile in PEST case with  $v_w = -0.2$  for different values of  $E$ .

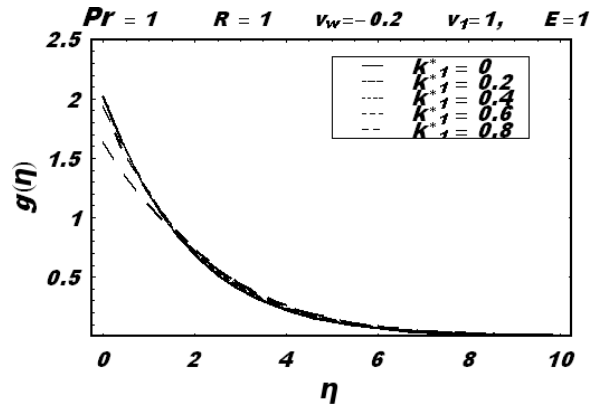


Fig. 17. Temperature profile in PEHF case with  $v_w = -0.2$  for different values of  $k_1^*$ .

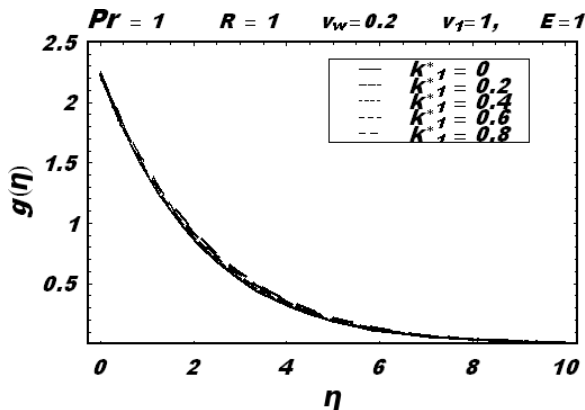


Fig. 16. Temperature profile in PEHF case with  $v_w = 0.2$  for different values of  $k_1^*$ .

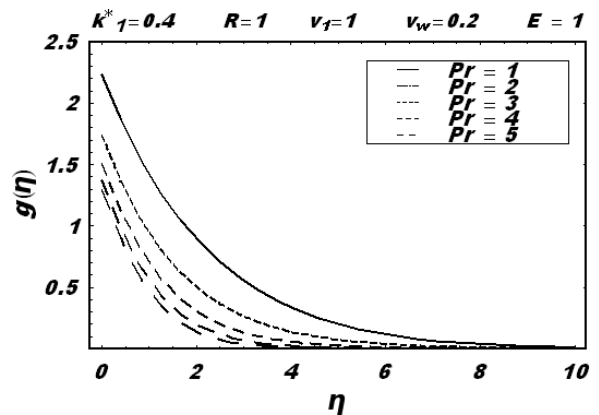


Fig. 18. Temperature profile in PEHF case for different values of  $Pr$ .

#### 4. Convergence and Discussion

The purpose of this section is to discuss the convergence and salient features of the series solutions. Here Figures 1–3 are plotted to ensure the convergence; it is found that  $-1.10 \leq \bar{h}_1 \leq -0.40$ ,  $-0.68 \leq \bar{h}_2 \leq -0.45$ , and  $-0.70 \leq \bar{h}_3 \leq -0.40$ . Figures 4–23 are sketched for the variations of several interesting flow parameters on velocity and temperature. The influence of  $k_1^*$  on  $f$  is shown in Figures 4 and 5. It is noticed that  $f$  decreases when  $k_1^*$  is increased. Furthermore,  $f_\eta$  also decreases for large value of  $k_1^*$  (Figs. 6 and 7). However, by increasing  $k_1^*$  the temperature profile in the PEST case increases (Figs. 8 and 9). The temperature in the PEST case is a decreasing function of  $Pr$  (Figs. 10 and 11). The variations of radiation parameter  $R$  and Eckert number  $E$  in PEST situation are shown in Figures 12–15. Here  $\theta$  is an increasing function

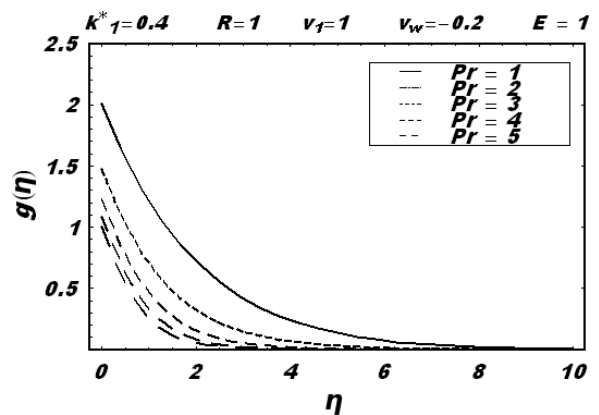


Fig. 19. Temperature profile in PEHF case for different values of  $Pr$ .

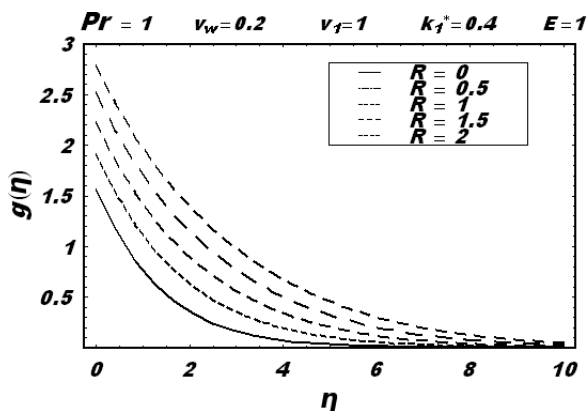
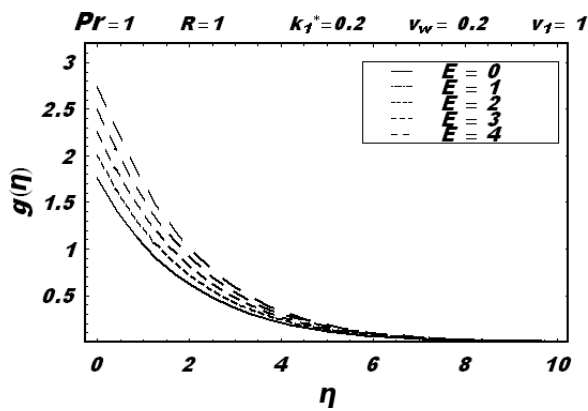


Fig. 20. Temperature profile in PEHF case for different values of radiation parameter  $R$ .



Figs. 22. Temperature profile in PEHF case for different values of radiation parameter  $E$ .

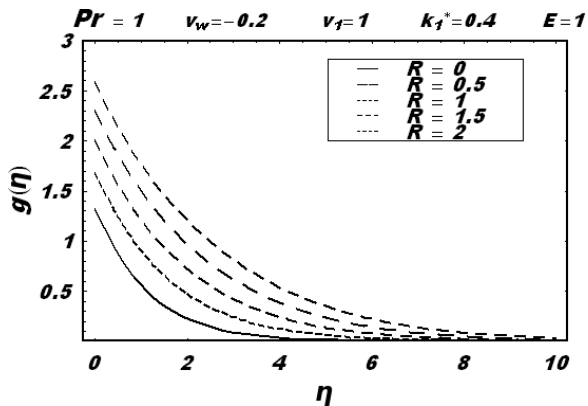
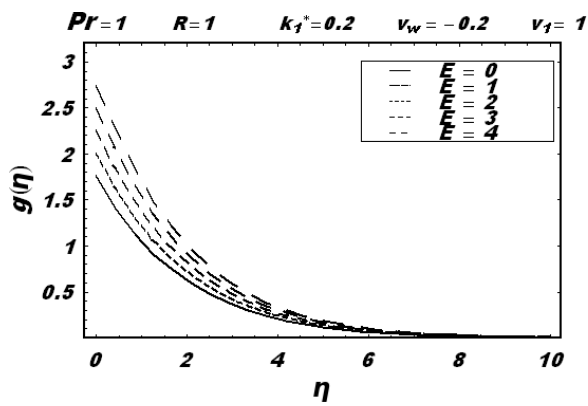


Fig. 21. Temperature profile in PEHF case for different values of radiation parameter  $R$ .



Figs. 23. Temperature profile in PEHF case for different values of radiation parameter  $E$ .

of  $R$  and  $E$ . Figures 16–23 are for variation of temperature in the PEHF cases. These figures show similar behaviour qualitatively as in the PEST case.

### 5. Closing Remarks

In this study, series solutions of velocity and temperature are constructed by a powerful analytic approach, namely, the homotopy analysis method (HAM). The problem for a porous and exponentially stretching

surface in PEST and PEHF cases is analyzed. The main points of the presented analysis are summarized as follows:

- The behaviour of  $Pr$  on  $\theta$  and  $g$  is quite opposite to that of  $E$ .
- The temperatures  $\theta$  and  $g$  are increasing functions of  $R$ ,  $E$ , and  $k_1^*$ .
- $f$  is a decreasing function of  $k_1^*$ .
- The corresponding series solutions of viscous fluid can be deduced by choosing  $k_0 = 0$ .



- [1] K. R. Rajagopal, *Acta Sin. Indica*. **18**, 1 (1982).
- [2] K. R. Rajagopal, On boundary conditions for fluids of the differential type. In: A. Sequeira (Ed.), *Navier-Stokes Equations and Related Non-Linear Problems*, Plenum Press, New York 1995, p. 273.
- [3] K. R. Rajagopal, A. Z. Szeri, and W. Troy, *Int. J. Nonlinear Mech.* **21**, 279 (1986).
- [4] C. Fetecau, D. Vieru, and C. Fetecau, *Int. J. Nonlinear Mech.* **43**, 451 (2008).
- [5] C. Fetecau and C. Fetecau, *Int. J. Eng. Sci.* **44**, 788 (2006).
- [6] D. Vieru, I. Siddique, M. Kamran, and C. Fetecau, *Comput. Math. Appl.* **56**, 1128 (2008).
- [7] W. C. Tan and T. Masuoka, *Int. J. Nonlinear Mech.* **40**, 515 (2005).
- [8] F. Shen, W. C. Tan, Y. H. Zhao, and T. Masuoka, *Appl. Math. Mech.* **25**, 1151 (2004).
- [9] I. Ahmad, M. Sajid, T. Hayat, and M. Ayub, *Comput. Math. Appl.* **56**, 1351 (2008).
- [10] T. Hayat, T. Javed, and Z. Abbas, *Int. J. Heat Mass Transf.* **51**, 4528 (2008).
- [11] Z. Abbas, T. Hayat, M. Sajid, and S. Asghar, *Math. Comput. Modelling* **48**, 518 (2008).
- [12] T. Hayat, S. Saif, and Z. Abbas, *Phys. Lett. A* **72**, 5037 (2008).
- [13] M. Sajid, I. Ahmad, T. Hayat, and M. Ayub, *Commun. Nonlinear Sci. Numer. Simul.* **14**, 96 (2008).
- [14] Z. Abbas, Y. Wang, T. Hayat, and M. Oberlack, *Int. J. Nonlinear Mech.* **43**, 783 (2008).
- [15] B. C. Sakiadis, *AIChE J.* **7**, 26 (1961).
- [16] B. C. Sakiadis, *AIChE J.* **7**, 221 (1961).
- [17] I. C. Liu, *Int. J. Heat Mass Transf.* **47**, 4427 (2004).
- [18] T. Hayat, Z. Abbas, and T. Javed, *Phys. Lett. A* **372**, 637 (2008).
- [19] T. Hayat, T. Javed, and Z. Abbas, *Nonlinear Anal.: Real World Appl.* **10**, 1514 (2009).
- [20] M. Sajid, *Nonlinear Dyn.* **50**, 27 (2007).
- [21] P. D. Ariel, *Comput. Math. Appl.* **54**, 920 (2007).
- [22] T. Hayat and T. Javed, *Phys. Lett. A* **370**, 243 (2007).
- [23] K. Vajravelu and J. R. Canon, *Appl. Math. Comput.* **181**, 609 (2006).
- [24] R. Cortell, *Int. J. Nonlinear Mech.* **41**, 78 (2006).
- [25] R. Cortell, *Phys. Lett. A* **357**, 298 (2006).
- [26] S. K. Khan and E. Sanjayanand, *Int. J. Heat Mass Transf.* **48**, 1534 (2005).
- [27] S. J. Liao, *Commun. Nonlinear Sci. Numer. Simul.* doi: 10.1016/j.cnsns.2008.04.013.
- [28] S. J. Liao and Y. Tan, *Studies Appl. Math.* **119**, 297 (2007).
- [29] S. J. Liao, Chapman & Hall/CRC Press, Boca Raton 2003.
- [30] S. J. Liao, *J. Fluid Mech.* **488**, 189 (2003).
- [31] S. J. Liao and I. Pop, *Int. J. Heat Mass Transf.* **47**, 75 (2004).
- [32] S. Abbasbandy, *Phys. Lett. A* **360**, 109 (2006).
- [33] S. Abbasbandy, M. Yurusoy, and M. Pakdemirli, *Z. Naturforsch.* **63a**, 564 (2008).
- [34] S. Abbasbandy, *Appl. Math. Model.* **32**, 2706 (2008).
- [35] S. Nadeem and M. Ali, *Commun. Nonlinear Sci. Numer. Simul.* doi: 10.1016/j.cnsns.2008.05.013.
- [36] M. Sajid, M. Awais, S. Nadeem, and T. Hayat, *Comput. Math. Appl.* **56**, 2019 (2008).
- [37] T. Hayat and T. Javed, *Phys. Lett. A* **370**, 243 (2007).
- [38] M. Sajid and T. Hayat, *Int. Commun. Heat Mass Transf.* doi: 10.1016/j.icheatmasstransfer.2008.08.010.
- [39] M. Sajid and T. Hayat, *Chaos, Solitons, and Fractals* **38**, 506 (2008).
- [40] T. Hayat and Z. Abbas, *Chaos, Solitons, and Fractals* **38**, 556 (2008).
- [41] R. L. Fosdick and K. R. Rajagopal, *Arch. Ration. Mech. Anal.* **70**, 145 (1979).
- [42] M. Q. Brewster, *Thermal Radiative Transfer and Properties*, Wiley, New York 1992.
- [43] M. Sajid, M. Awais, S. Nadeem, and T. Hayat, *Comput. Math. Appl.* **56**, 2019 (2008).
- [44] S. Nadeem and M. Awais, *Phys. Lett. A* **372**, 4965 (2008).
- [45] S. Nadeem and M. Ali, *Commun. Nonlinear Sci. Numer. Simul.* **14**, 2073 (2009).